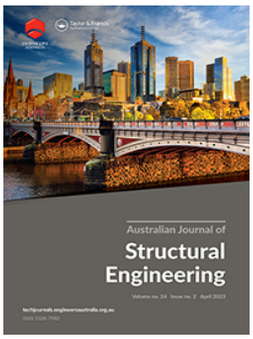

Australian Journal of Structural Engineering

ISSN: (Print) (Online) Journal homepage: https://www.tandfonline.com/loi/tsen20

Structural reliability and partial safety factor assessment of unreinforced masonry in vertical bending

Andrea C. Isfeld, Mark G. Stewart & Mark J. Masia

To cite this article: Andrea C. Isfeld, Mark G. Stewart & Mark J. Masia (2023): Structural reliability and partial safety factor assessment of unreinforced masonry in vertical bending, Australian Journal of Structural Engineering, DOI: 10.1080/13287982.2023.2173868

To link to this article: https://doi.org/10.1080/13287982.2023.2173868

Published online: 17 Feb 2023.

AUSTRALIAN JOURNAL OF STRUCTURAL ENGINEERING
https://doi.org/10.1080/13287982.2023.2173868

Structural reliability and partial safety factor assessment of unreinforced masonry in vertical bending

Andrea C. Isfeld, Mark G. Stewart and Mark J. Masia

School of Engineering, Research Associate, Centre for Infrastructure Performance and Reliability, the University of Newcastle, Newcastle, New South Wales, Australia

ABSTRACT

This paper focuses on a structural reliability-based assessment of clay brick unreinforced masonry (URM) walls subjected to uniformly distributed out-of-plane loads in one-way vertical bending. Stochastic models combining finite element analysis (FEA) and Monte Carlo simulations (MCS) are used to account for spatial variability of the flexural tensile bond strength when estimating the wall failure loads. The strength of URM walls is known to be influenced by the flexural tensile bond strength, which is subject to high spatial variability as batching, workmanship, and environmental exposure alter the strength of this bond. For this assessment, single skin walls have been considered with bond strength statistics seen in typical construction. The model error statistics available for similar walls are combined with the results of the spatial stochastic FEA and probabilistic load models to determine the reliability index corresponding to the Australian Standard for Masonry Structures AS 3700 design of members in vertical bending. It was found that existing levels of reliability exceed target reliabilities, and the capacity reduction factor can be increased from 0.60 to 0.65 for URM walls in one-way vertical bending while still providing an acceptable level of reliability. A sensitivity analysis showed this finding to be robust.

ARTICLE HISTORY
Received 01 March 2022
Accepted 24 January 2023

KEYWORDS
Unreinforced masonry; spatial variability; structural reliability; out-of-plane loading; vertical bending; finite element modelling; Monte Carlo simulation; code calibration

1. Introduction

To determine the strength of an unreinforced masonry (URM) wall subjected to one-way vertical bending the Australian Standard for Masonry Structures (AS 3700 2018) follows a limit states (or load and resistance factor design or LRFD) approach, whereby the moment resistance is based on the fifth-percentile (characteristic) value of flexural tensile bond strength (f'_{mt}). The capacity reduction factor for flexure has been $\phi = 0.6$ since the first limit states standard was released in 1988, based on a calibration with the earlier working stress code. However, there has been no reliability-based calibration of URM walls in flexure in Australia, nor internationally as far as the authors are aware. On the other hand, a reliability-based approach was used by Lawrence and Stewart (2009) who found that the capacity reduction factor for URM walls loaded in compression can be increased from 0.45 to 0.75, and this was incorporated into AS 3700. Reliability-based calibration of the Australian Concrete Structures Code (2018) has resulted in Φ values increasing from 0.6 to 0.65 for axial loading, from 0.70 to 0.75 for shear, and from 0.8 to 0.85 for flexure (Stewart et al. 2016; Argarwal, Foster, and Stewart 2021). It is unclear if the capacity reduction factor for URM walls in flexure may also be increased – this is the motivation for the present paper.

In masonry walls, the unit–mortar interface is a plane of weakness and dictates the points at which flexural failure initiates, governed by the flexural tensile bond strength. This bond is subject to high spatial variability as it is affected by batching, workmanship, and environmental exposure. This means that adjacent mortar joints between bricks (units) may have significantly different material properties, and hence high spatial variability.

A random field FEA was developed to include spatial variability in linear and non-linear structural systems by Liu et al. (1986). Variability can be introduced at the level of material properties, geometry, or loads, and the effect is measured on the response of the system. Versions of this approach are also referred to as the stochastic finite element method (SFEA), the random finite element method, or the probabilistic finite element method (Aggregui-Mena, Margetts, and Mummery 2016). Moradabadi et al. (2015) utilised the random field finite element method for the analysis of eccentrically loaded masonry piers, showing agreement with physical testing. A similar approach was applied by Isfeld et al. (2016) for the simulation of grout injection in historic stone masonry walls. Li et al. (2014) modelled brick masonry walls under one-way bending due to uniform pressure loads with unit-to-unit stochastic spatial variability and

CONTACT Andrea C. Isfeld andrea.isfeld@newcastle.edu.au

compared the results with a nonspatial stochastic analysis whereby a single random value was used for all joints in the wall. A nonspatial analysis was found to overestimate the probability of wall failure compared to spatial analysis, demonstrating the importance of considering the unit-to-unit spatial variability of flexural bond strength. Li et al. (2016) utilised SFEA to model the behaviour of brick panels, considering spatial variability of the mortar joint properties at different levels of correlation. Statistical independence was considered between joints, with the unit-to-unit spatial correlation coefficient $\rho = 0$ and a realistic correlation of $\rho = 0.4$ (Heffler et al. 2008). Comparison of non-spatial ($\rho = 1$) stochastic FEA results, spatial stochastic FEA with $\rho = 0.4$, and the results of 310 experimental specimens showed improved agreement between the FEA and test results when the bond strength was spatially variable (Li et al. 2016). This is consistent with the conclusions of Li, Masia, and Stewart (2017) when applying the same modelling approach to walls subjected to two-way bending. Using this technique, Isfeld, Stewart, and Masia (2021) compared spatial SFEA and test results of 2/3 scale brick walls 1, 2, 4 and 10 units long tested in one-way vertical bending. The walls were constructed by 10 different masons, and 10 corresponding sets of spatial SFEA were developed for each mason. Comparison with test results was used to probabilistically characterise model error for each wall length (Isfeld, Stewart, and Masia 2021).

Calibration of the capacity reduction factor for one-way bending in AS 3700 (2018) has been considered using several approaches. Stewart and Lawrence (2002) developed a structural reliability model for URM walls in one-way vertical bending. The analytical model considered first cracking, and the potential for redistribution of stresses until collapse through simplifying assumptions, and model error was ignored. A baseline lifetime reliability index (β) of 4.92 was obtained, and it was found that the reliability index was relatively insensitive to wall lengths exceeding about 10 units, and also relatively insensitive to wall height. The reliability index is related to the probability of failure by the inverse of the standard normal distribution function, with a higher reliability index indicating a lower probability of failure. Lawrence and Stewart (2011) conducted a reliability analysis on URM in one-way bending, utilising a database of 118 masonry wall tests to quantity model error (model uncertainty) for the AS 3700 design model. Considering a conservative lifetime target reliability index of $\beta_T = 4.3$ it was determined that the capacity reduction factor may need to be decreased slightly. However, no allowance was made for spatial variability of flexural strength, and it was concluded that 'It is possible that a more accurate behaviour model, which takes into account spatial variability and load sharing between units, could be used in combination with a higher capacity reduction factor to achieve the target reliability' (Lawrence and Stewart 2011). Following the updated wind loading statistics and target reliabilities, Stewart and Masia (2019) utilised the results of spatial stochastic FEA in a reliability-based calibration of the capacity reduction factor for URM in one-way bending and found evidence to support an increase of ϕ from 0.6 to 0.65. However, the authors address the need to accurately quantify model error statistics to improve the robustness of this study.

This paper focuses on a structural reliability-based assessment of clay brick URM walls subjected to uniformly distributed out-of-plane loads in one-way vertical bending. For the present design situation, this is a single skin infill masonry panel subject to a lateral (wind) load – i.e., there is no vertical pre-compression other than panel self-weight. This is a common structural scenario for URM walls in many forms of construction and one for which such walls are vulnerable to collapse under out-of-plane loading. Stochastic models combining FEA and MCS account for spatial variability of the flexural tensile bond strength when estimating the walls failure loads. Model error statistics are combined with the results of the spatial stochastic FEA and probabilistic load models to determine the reliability index corresponding to the Australian Standard for Masonry Structures AS 3700 (2018) design of members in vertical bending and to determine the capacity reduction factor required to meet the target reliability index.

2. Spatial Stochastic FEA Modelling

Spatial stochastic FEA modelling was completed for full-scale masonry walls 10 units long (2400 mm), 28 units tall (2408 mm) and 110 mm thick, subjected to one-way vertical bending as shown in Figure 1. There is no vertical pre-compression other than panel self-weight. The bricks are modelled as solid expanded half units (two half units 120 × 110 × 86 mm (length × width × height) make up each 240 mm long brick unit) accounting for the mortar joint thickness (10 mm) using the simplified micro-modelling approach (Lourenço, Rots, and Blaauwendraad 1995; Lourenço 1996; Lourenço and Rots 1997). The DIANA (2017) finite element software is utilised here for its ability to simulate a range of masonry behaviour. Half units are assigned linear elastic material properties with non-linear behaviour allocated to the mortar joint and unit crack interface elements. The combined cracking-shearing-crushing model is used to model the mortar joints Lourenço, Rots, and Blaauwendraad (1995), Lourenço and Rots (1997). This model captures tensile, shear, and crushing fracture, as well as frictional slip. Discrete cracking

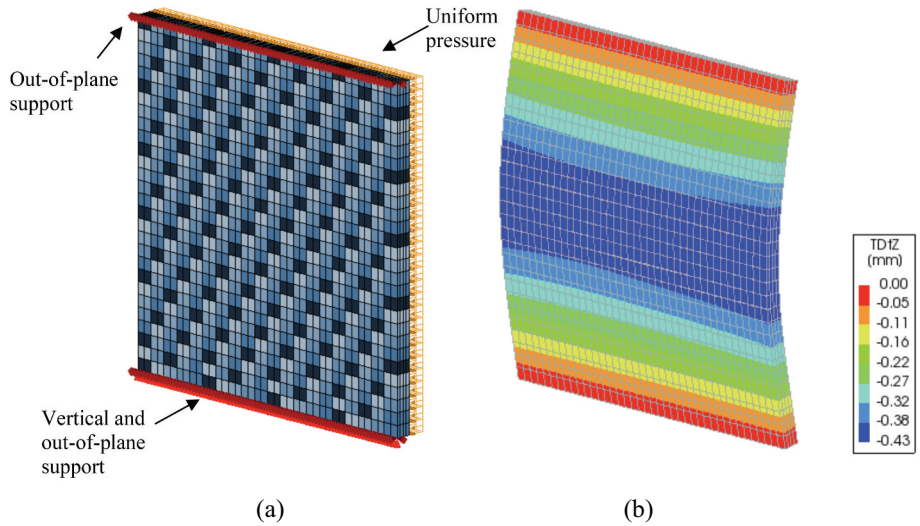

Figure 1. FEA of URM in vertical one-way bending (a) model (b) typical out-of-plane displacement at peak load.

using the linear tensile softening model is included using interface elements to simulate mid-length unit cracking. Mortar joint failure in tension and shear can be simulated, along with unit tensile failure, and combined mortar/unit shear and compressive failure. The spatial stochastic FEA includes unit-to-unit spatial variability of flexural tensile bond strength according to the approach developed and validated by Heffler (2009) and evaluated further by Li et al. (2014); Li et al. (2016); Li, Masia, and Stewart (2017) and Isfeld, Stewart, and Masia (2021). Heffler et al. (2008) found that the bond strength is best represented by a normal distribution, truncated at zero, having unit-to-unit spatial correlation of 0.4 within each course and no correlation (statistically independent) between courses. Figure 2 shows the spatial variability of bond strength and cracking at peak load for a typical wall (Isfeld, Stewart, and Masia 2021).

2.1. FEA Model Assembly

The boundary conditions are consistent with standard construction practice and representative of walls with no axial precompression. The bottom course of a masonry wall would typically be in contact with a concrete footing, or damp-proof course, both of which result in reduced bond strength. Thus, the conservative assumption of zero bond strength is made, and the unloaded edge of the first course is restrained against vertical and out-of-plane displacement as shown in Figure 1 (a) with rotation permitted about the support. This approach is aligned with the recommendation in AS 3700 (2018) to consider the bond

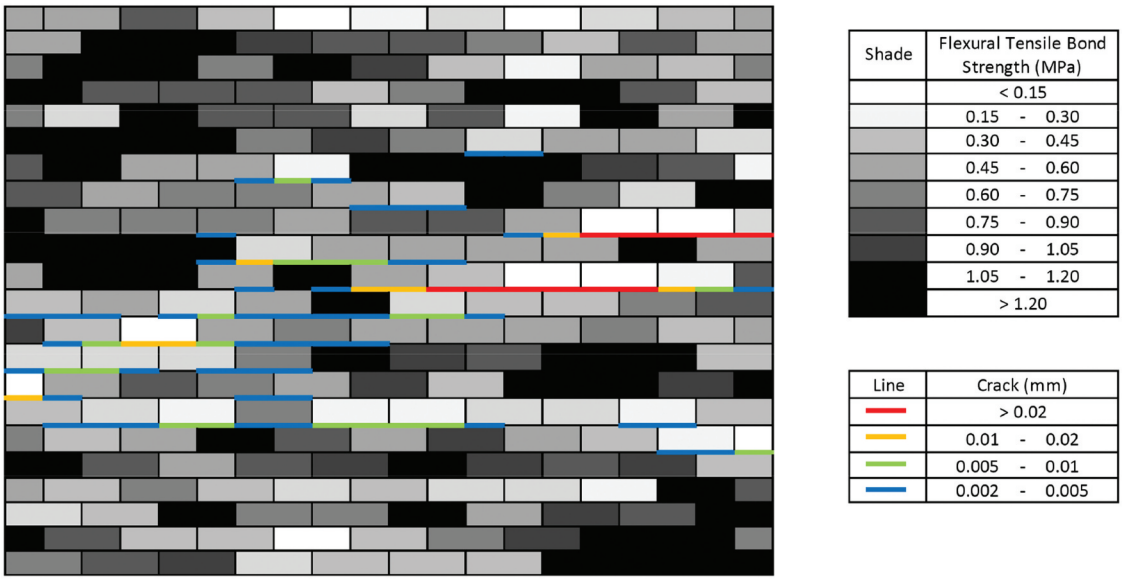

Figure 2. Example of tension face cracking pattern and bond strength distribution at peak load (adapted from Isfeld, Stewart, and Masia 2021).

strength as zero when interfacing with other materials. Out-of-plane displacements are similarly restricted to the unloaded edge at the top of the wall, representing a stiff diaphragm. In-plane displacements are restricted at a single node on each support to prevent rigid body movement. The walls are modelled with self-weight and uniform out-of-plane pressure is applied to the full wall as shown in Figure 1 (a). Analysis procedures and mesh refinement assessed by Isfeld, Stewart, and Masia (2021) are used in all models. The out-of-plane displacement is recorded at the centre of the unloaded face (height/2, length/2) for each load step and used to establish the load–displacement behaviour of each model.

2.2. Material Properties

The material properties are categorised as deterministic, spatially variable, and spatially dependent. The flexural tensile strength of the unit–mortar interface is the most critical material parameter for determining the load resistance of masonry walls subjected to one-way vertical bending (Stewart and Lawrence 2002, Heffler 2009). This value is subsequently treated as spatially variable, varying along the length and height of the wall on a unit-to-unit basis, and directly converted to a direct tensile bond strength value. Cohesion, fracture energy, and in some cases compressive strength are treated as spatially dependent variables, calculated as a function of the direct tensile strength. The fracture energy is also known to significantly influence the moment redistribution between units, and the subsequent load resistance of the walls (Heffler 2009). In turn, cohesion and compression strength are adjusted to ensure compatibility with the composite interface model criterion (DIANA 2017). The remaining material parameters are deterministic based on representative average values as outlined by Heffler (2009), and Li et al. (2014); Li et al. (2016); Li, Masia, and Stewart (2017) and Isfeld, Stewart, and Masia (2021).

A program was written in MATLAB to automate the procedure of batching the FEA simulations with spatially variable material properties. This program would output a python script based on the wall dimensions, stochastic material properties, and number of simulations in the MCS. For each model the first step is to assign a statistically independent tensile bond strength to the mortar joint below the first unit in each course of masonry. Next, the adjacent joint within each course is assigned a tensile bond strength that is correlated to the first joint. This pairwise correlation is completed for the remaining mortar joints in each course. Spatially dependent variables are similarly assigned. All head (perpend) joints are assumed statistically independent, and no unit-to-unit correlation is included.

2.2.1. Flexural Tensile Bond Strength

The probability distribution of the flexural tensile bond strength used in these simulations was based on testing completed by McNeilly et al. (1996) for 17 building sites in Melbourne and by Heffler et al. (2008) on full-scale wall samples. Consideration is also made for the characteristic strength values in AS 3700 (2018).

McNeilly et al. (1996) completed bond wrench testing at 19 building sites in Australia. To obtain samples that were representative of typical construction, arrangements were made such that the tested brickwork had already been constructed when agreement was made to carry out testing. The samples were tested a minimum of 7 days after construction. Samples taken from two building sites were cured using enhanced techniques and were excluded from this analysis. Mortar composition was analysed to assess the accuracy of batching. Of 75 wet mortar samples, 33 contained no lime, five contained less than 0.10 parts by volume, and the remaining mortars varied between 0.12 and 1.12 parts. The cement content varied between the test sites with the highest cement content 1:0:4.2 (cement:lime:sand proportions by volume) and the lowest 1:0:12.7. No admixtures were added to the mortar. McNeilly et al. (1996) reported the mean and COV of flexural tensile bond strength for each site; the mean ranged from 0.21 to 0.85 MPa (mean of 0.52 MPa) and the COV from 0.16 to 0.49 (mean of 0.30). The overall mean and COV of all test sites are 0.52 MPa and 0.50, respectively. McNeilly et al. (1991) considered a normal distribution as providing best fit for the data. McNeilly et al. (1991) noted that a log-normal or Weibull distributions could be suitable alternatives as described by Lawrence (1983, 1985).

Heffler et al. (2008) completed bond wrench testing on all mortar joints in four laboratory constructed brick masonry walls. The walls were constructed by four different masons with a range of experience levels to assess the variability of workmanship. Two mortar mixes were tested, 1:1:6 (cement:lime:sand proportions by volume) with no admixtures and 1.5:1:6 which included an air entraining agent to improve workability. Typical extruded clay bricks were used to construct all walls. The walls were constructed over 2 days and cured between 28 and 40 days prior to testing. The overall mean and COV of all bond strengths for walls constructed with mortar not containing admixtures were found to be 0.53 MPa and 0.50, respectively.

In principle, the statistics for flexural tensile strength may also need to be adjusted to account for variability in flexural tensile strength test procedures. The accuracy of the bond wrench test is influenced by the placement of the apparatus and the skill of the operator, and so the variability of flexural tensile strength is likely to be overestimated. Nonetheless, this source of variability is

not factored out of the analysis. This approach is consistent with the strength statistics for concrete, reinforcement and other materials used in reliability-based calibration, even though it is recognised that the variability of the test procedure for flexural tensile strength is likely to be higher than most other test procedures. Conservatively, no adjustment was made to the statistics used for flexural bond strength.

Hence, conservative flexural tensile strength statistics are a mean of 0.52 MPa and a COV of 0.5 normally distributed with the COV representing the upper end of variabilities to be expected for an individual site or wall. This is the benchmark scenario representing a worst case, denoted as Case 1. A sensitivity analysis to be discussed later will assess the effect of Weibull and lognormal distributions in structural reliability.

The Australian Standard for Masonry Structures AS 3700 (2018) recommends a characteristic flexural tensile bond strength not greater than 0.2 MPa for clay, concrete, and calcium silicate masonry (excluding special masonry). The 5th percentile (characteristic) value for Case 1 is 0.14 MPa, which will lead to a more conservative design. If the characteristic strength value is taken as 0.2 MPa with a COV of 0.5, this corresponds to a mean flexural tensile bond strength value of 0.746 MPa. These statistics will lead to significantly higher reliabilities and will be discussed later in the paper. However, if a lower COV of 0.3 is assumed, which represents the mean reported value from McNeilly et al. (1996), then the mean flexural tensile bond strength value reduces to 0.395 MPa, this will be analysed as Case 2.

All cases considered a unit-to-unit correlation of 0.4 within each course and no correlation between courses (Heffler et al. 2008) for the bed joints. No data is available on the spatial variability of the head joint (perpend joint) bond strength, and thus no correlation was considered in the variation of these values ($\rho = 0$). Flexural tensile bond strengths were converted to direct tensile strengths by dividing by a factor 1.5 (Petersen et al. 2012) as indicated in. This is consistent with the approach used for plain concrete in AS 3600 (2018), and experimentally by Raphael (1984) and Van der Pluijm (1997).

2.2.2. Other Material Properties

Material properties used in Isfeld, Stewart, and Masia (2021) are based on those outlined by Heffler (2009) and evaluated further by Li et al. 2014; Li et al. (2016); Li, Masia, and Stewart (2017) have been used here and are shown in Table 2. All brick properties including Young's modulus, Poisson's ratio, and density, as well as brick tensile strength values are modelled as deterministic. High values for the linear normal and tangential stiffness modulus were set to maintain the continuity of brick displacements across the interface. The tensile fracture energy and cohesion are calculated from the flexural tensile strength values, all other mortar joint properties represent average (deterministic) values used across all models. The tensile fracture energy for the mortar joints, G_f^I (N/mm), is related to the direct tensile strength, f_t (MPa), using Equation (1) established by Heffler (2009) using a best fit relationship for test data with direct tensile bond strengths up to 0.8 MPa from Van Der Pluijm (1997).

$$G_f^I = 0.01571 f_t + 0.0004882 \tag{1}$$

The interface cohesion, c, is related to the tensile bond strength outlined by Milani and Lourenço (2013).

$$c = 1.4 f_t \tag{2}$$

The residual cap must fall outside the tension cut off for all direct tensile strength values. To enforce this, the compressive strength of masonry is increased to 25 MPa for $f_t > 1.4$ MPa and to 30 MPa for $f_t > 1.7$ MPa.

2.3. Wall Length

The length of a masonry wall subjected to one-way vertical bending is known to affect the ultimate strength of the wall (Baker 1981; Isfeld, Stewart, and Masia 2021) and has subsequently been shown to affect the reliability (Stewart and Lawrence 2002). Baker (1981) tested 2/3 scale brick wall panels under out-of-plane loading and observed that the strength increased with increasing wall length for lengths up to 4 units but then decreased for longer panels. Isfeld, Stewart, and Masia (2021) simulated this testing using spatial stochastic FEA for walls 1 to 15 units long and 24 units tall and found that the wall strength began to stabilise beyond seven units.

Several hypotheses exist to describe the influence of bond strength variability on the ultimate strength of URM walls in one-way vertical bending, including the weakest link, brittle/parallel system (successive cracking), partial plasticity, and full plasticity (averaging) (Baker 1981, Stewart and Lawrence 2002). The weakest link hypothesis predicts failure will occur once a single joint strength has been exceeded, while the parallel systems hypothesis permits progressive redistribution of load after cracking until the remaining joints cannot sustain the load. The partial plasticity hypothesis assumes that averaging of joint strengths is limited to some number, N, of adjacent joints. Thus, failure of a wall is initiated when the mean moment resistance of the lowest strength N adjacent joints is exceeded. Stewart and Lawrence (2002) utilised the parallel system hypothesis to predict the strength of masonry walls of varied length, height, and thickness, finding that reliability is insensitive to the length as for longer walls even though cracking must progress over a greater number of units. Comparison of the parallel system hypothesis with the weakest link and averaging hypothesis showed

Table 1. Flexural tensile bond strength properties and wall length.

Case	Mean	COV	5th Percentile (f_{mt})	Distribution	Wall Length
1	0.520 MPa	0.50	0.14 MPa	Truncated Normal	2400 mm
2	0.395 MPa	0.30	0.20 MPa	Truncated Normal	2400 mm
3	0.520 MPa	0.50	0.14 MPa	Truncated Normal	1200 mm
4	0.520 MPa	0.50	0.14 MPa	Truncated Normal	3600 mm

that the weakest link was overly conservative, while the averaging hypothesis was nonconservative. Baker (1981) found the partial plasticity hypothesis with N = 3 or 4 to best fit the experimental data, and this was in agreement with the findings of Isfeld, Stewart, and Masia (2021).

Individual low strength joints have a significant effect on the strength of narrow wall panels and can be found to initiate failure. Whereas in longer wall panels some averaging of adjacent joint strengths reduces the effect of an individual low strength joint. The influence of the wall length on the reliability is studied by increasing and decreasing the wall length by 50%. In Case 3 the wall length is 5 units (1200 mm), while in Case 4 the

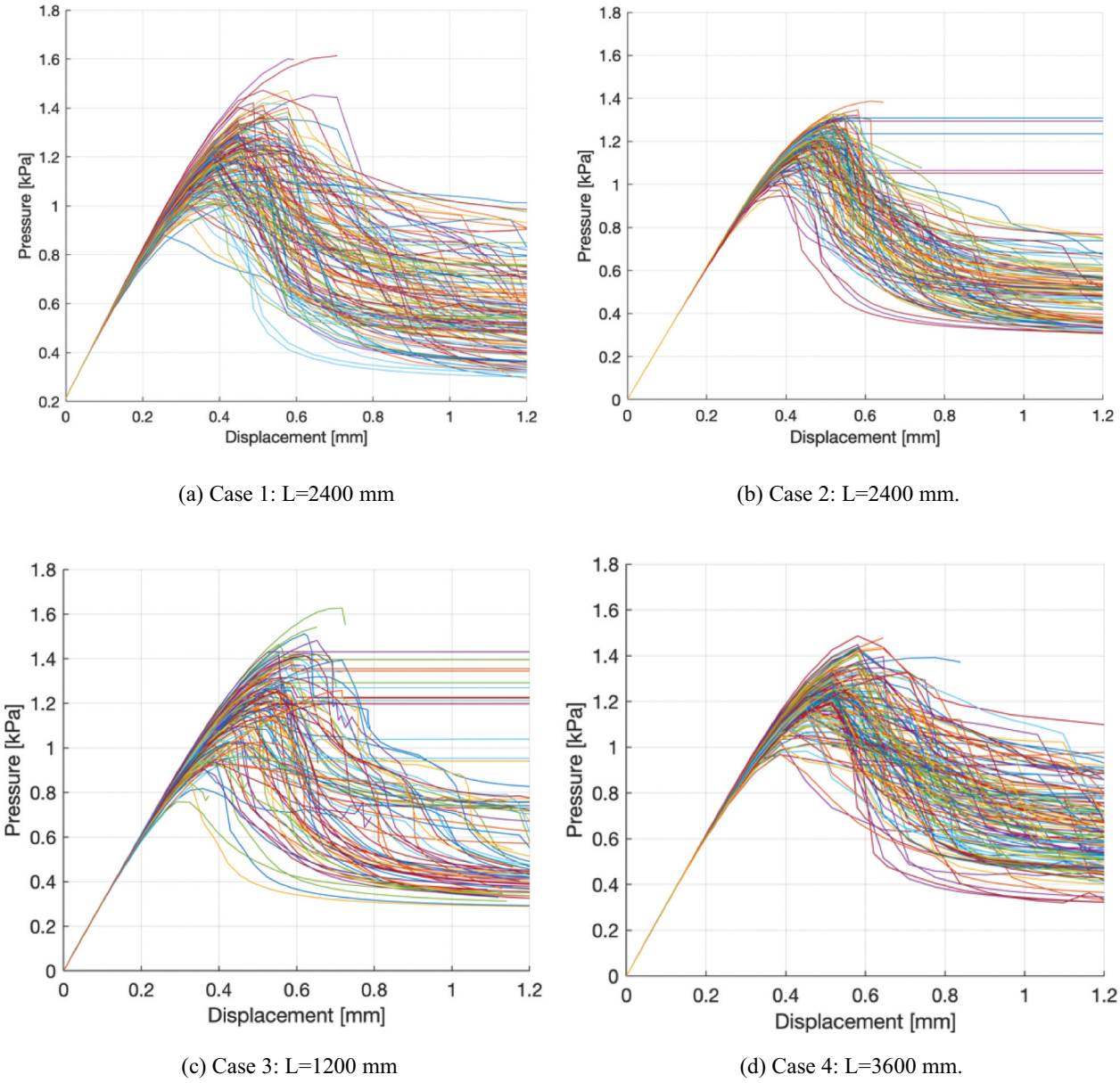

(a) Case 1: L=2400 mm

(b) Case 2: L=2400 mm.

(c) Case 3: L=1200 mm

(d) Case 4: L=3600 mm.

Figure 3. Load displacement behaviour for Cases 1–4.

Table 2. FEA material data for deterministic analysis.

Material		Units	Model Input	Source
Brick	Young's Modulus	N/mm^2	20 000	Heffler (2009)
	Poisson's Ratio	-	0.15	
	Density	kg/mm^3	1800	
Brick Crack Fictitious Values	Linear normal stiffness modulus	N/mm^3	1000	(Heffler 2009)
	Linear tangential stiffness modulus	N/mm^3	1000	
	Direct tensile strength	N/mm^2	2	
	Tensile fracture energy	Nmm/mm^2	0.5	
Mortar Joints	Linear normal stiffness modulus	N/mm^3	353	Heffler (2009)
	Linear tangential stiffness modulus	N/mm^3	146	Heffler (2009)
	Flexural tensile strength	N/mm^2	Table 1	
	Direct tensile strength	N/mm^2	$f'_{mt}/1.5$	(Petersen et al. 2012)
	Tensile fracture energy	Nmm/mm^2	Eq. (1)	Heffler (2009)
	Cohesion	N/mm^2	Eq. (2)	Milani and Lourenço (2013)
	Tangent friction angle	-	0.75	Heffler (2009)
	Tangent dilatancy angle	-	0.6	Heffler (2009)
	Tangent residual friction angle	-	0.75	Heffler (2009)
	Confining normal stress	N/mm^2	−1.2	Heffler (2009)
	Exponential degradation coefficient	-	5	Heffler (2009)
	Capped critical compressive strength	N/mm^2	20	Heffler (2009)
	Shear traction control factor	-	9	Heffler (2009)
	Compressive fracture energy	Nmm/mm^2	15	Heffler (2009)
	Equivalent plastic relative displacement	-	0.012	Heffler (2009)
	Shear fracture energy factor	-	0.15	Heffler (2009)

Table 3. Statistical parameters for reliability analysis.

Parameter	Mean	COV	Distribution	Source
Ultimate Resistance R_u	1.21 kPa	0.11	Normal	Case 1 spatial stochastic FEA
	1.19 kPa	0.07	Weibull	Case 2 spatial stochastic FEA
	1.20 kPa	0.11	Normal	Case 3 spatial stochastic FEA
	1.24 kPa	0.09	Normal	Case 4 spatial stochastic FEA
Self-weight, γ	19 kN/m^3	0.02	Normal	Lawrence and Stewart (2009)
Model Error, ME	0.95	0.14	Normal	Isfeld, Stewart, and Masia (2021)

wall length is 15 units (3600 mm). These cases are also based on Case 1 material properties, see Table 1.

2.4. Spatial Stochastic FEA Results for Ultimate Resistance R_u

A total of 150 spatial stochastic FEA Monte Carlo simulations (MCS) were completed for each case where convergence for mean and COV were observed, and also to give a sample size sufficient for probabilistic model fitting. Failure was characterised by mid-height cracking, and load–displacement behaviour for all cases is shown in Figure 3. Load redistribution occurs as cracking progresses along the wall length; this is seen as a gradual reduction in post-peak loading, in some simulations rapid failure results in failure to converge (plot terminates), or significant rigid body displacement as a hinge is formed (rapid increase in horizontal displacement, beyond which the solution diverges).

The statistics of mean peak pressure values (R_u) are shown in Table 3. The method of maximum likelihood is an alternative method for statistical parameter estimation, which is observed to yield a better fit for larger sample sizes. However, in this case, the method of maximum likelihood yielded near identical 'best fit' statistical parameters to those obtained from the method of moments.

The results of the spatial stochastic FEA are compared to five different distribution types: normal, log-normal, Weibull, Gumbel, and gamma. The Kolmogorov–Smirnov (KS) test was applied at the 5% significance level to test the hypothesis that the FEA results are represented by the specified distributions. For all cases, the KS test failed to reject the null hypothesis for all distributions. As shown in Figures 4, 6, and 7 for Cases 1, 3, and 4 the Weibull distribution appears to overestimate the likelihood of low strength values and the normal distribution provides the closest fit (as it sits very near to the perfect-fit line given for

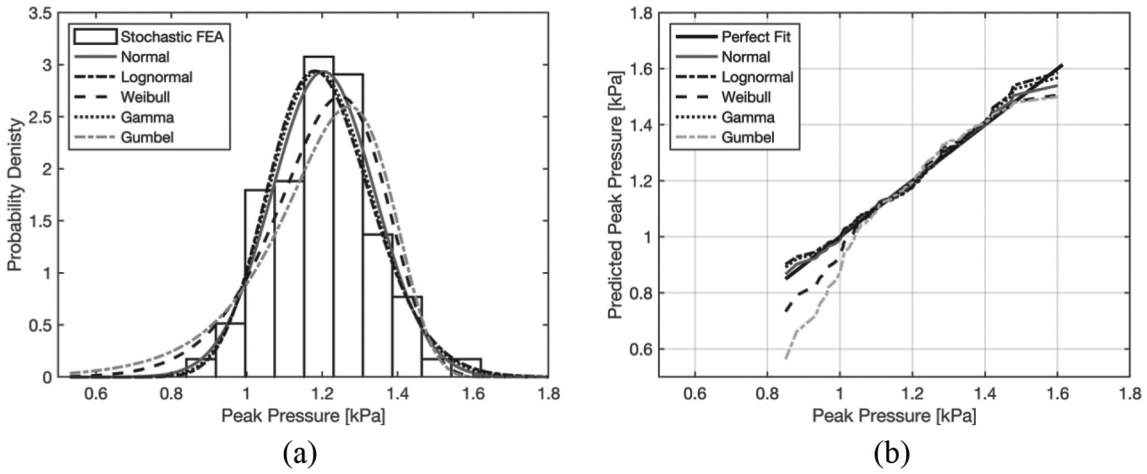

Figure 4. Case 1 (a) probability distribution of spatial stochastic FEA peak pressure (b) inverse CDF plot of spatial stochastic FEA peak pressure.

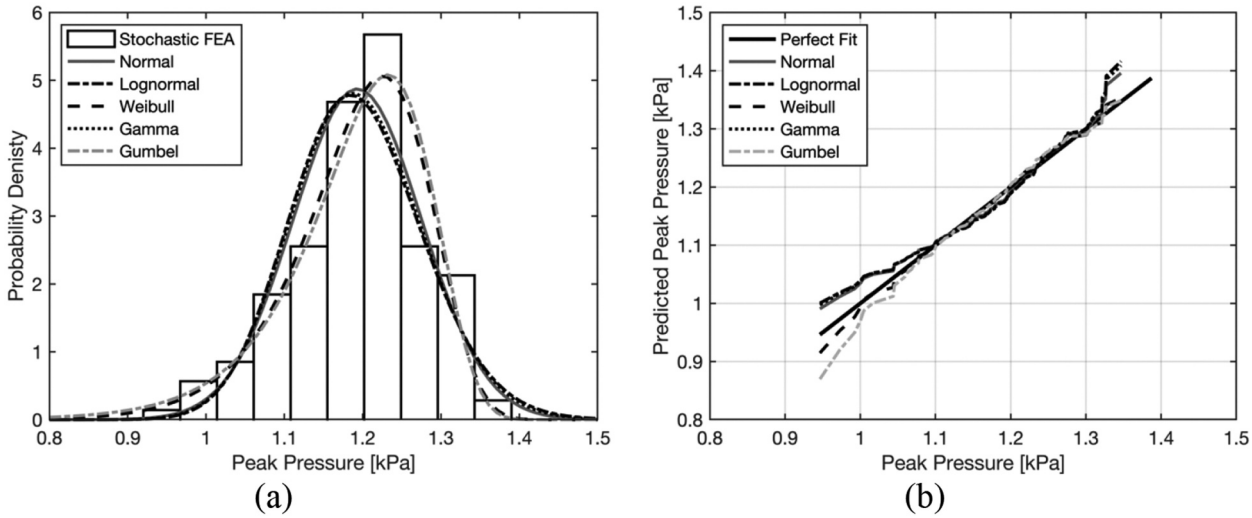

Figure 5. Case 2 (a) probability distribution of spatial stochastic FEA peak pressure (b) inverse CDF plot of spatial stochastic FEA peak pressure.

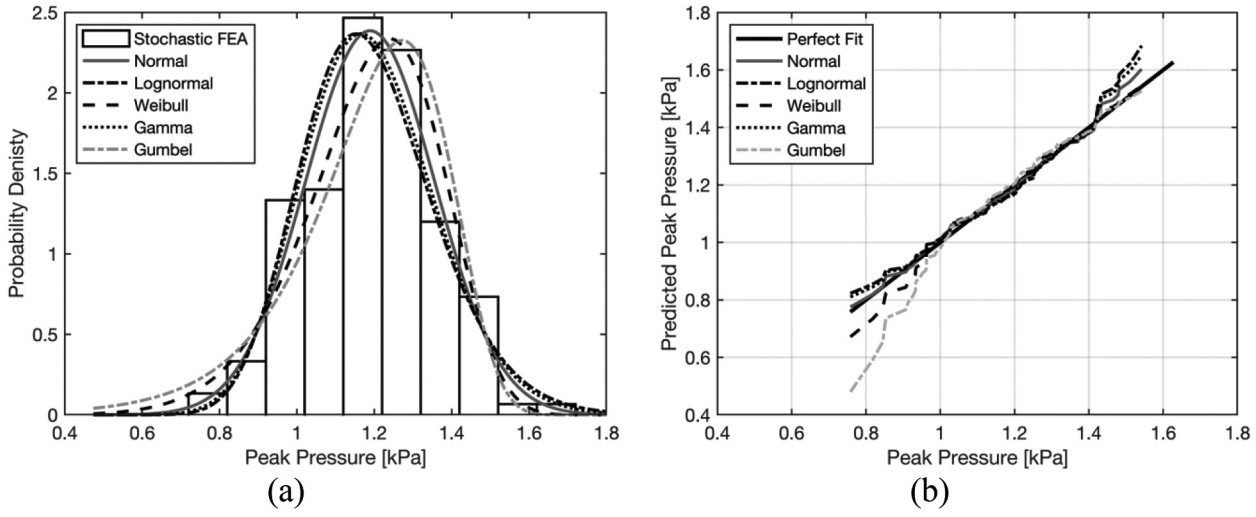

Figure 6. Case 3 (a) probability distribution of spatial stochastic FEA peak pressure (b) inverse CDF plot of spatial stochastic FEA peak pressure.

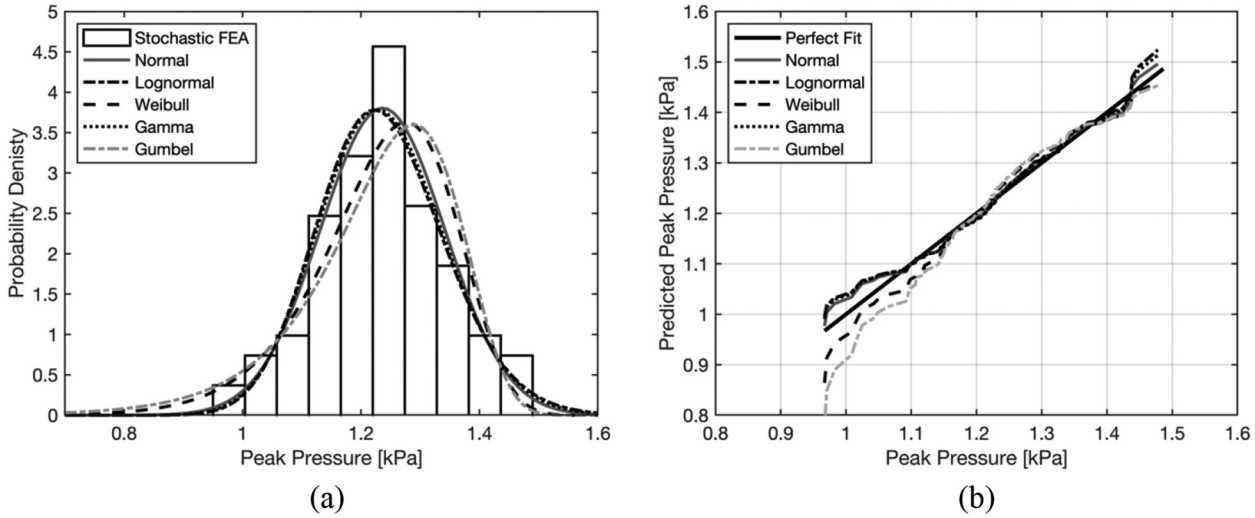

Figure 7. Case 4 (a) probability distribution of spatial stochastic FEA peak pressure (b) inverse CDF plot of spatial stochastic FEA peak pressure.

the cumulative distribution function (CDF)). The same is true for Case 2 shown in Figure 5, however the overestimation of low strength values provided by the Weibull distribution is minimal, while the remaining distributions (excluding Gumbel) significantly underestimate the low strength values. The normal distribution is selected, as it is slightly conservative, for Cases 1, 3, and 4, and the Weibull distribution is selected for Case 2.

2.5. SFEA Model Error

The model error (or model uncertainty) statistics were established through comparison of the SFEA results with the experimental failure loads of 10 simply supported brick masonry walls in one-way vertical bending. The mean model error (ME) is calculated as the ratio of the mean experimental results to the mean model prediction. The walls studied were constructed using 2/3 scale bricks and were 1–10 units long and 22 units tall and constructed by 10 different masons, for more details see Baker (1981). These test results were then compared with spatial stochastic finite element models using the same techniques as that used in the present study. The model error for a 10 unit length wall (the same configuration as Case 1) was mean and COV of 0.95 and 0.14, respectively, normally distributed Isfeld, Stewart, and Masia (2021). For a shorter length wall of four units, the mean model error increased to 1.10 Isfeld, Stewart, and Masia (2021). As no experimental walls exceeded 10 units in length a model error for 15 units (Case 4) was not calculated. Hence, to be conservative, the model error for a 10 unit length wall is applied for all wall lengths herein, see Table 3.

3. Structural Reliability Analysis

Reliability analysis based on MCS is used to evaluate the current capacity reduction factors for one-way vertical bending in AS 3700 (2018). A calibration of the capacity reduction factors is then completed, considering target reliability factors based on the Australian Standard AS 5104 (2017) and the Joint Committee on Structural Safety Probabilistic Model Code (JCSS 2021). Finally, a sensitivity analysis is completed to evaluate the critical assumptions used in the reliability analysis.

3.1. Structural Reliability

The probability that loading will exceed the structural resistance is defined as:

$$p_f = Pr[G(X) \leq 0] = Pr[R - S \leq 0] = \Phi(-\beta) \quad (3)$$

$$\beta = -\Phi^{-1}(p_f) \quad (4)$$

where G(X) is a limit state function describing the performance of a structure in terms of a vector of variables X. The actual resistance, R, and actual loading effects, S, are used to assess the probability of failure, p_f. A value of $G(X) \leq 0$ indicates failure. The reliability index, β, is calculated using the inverse of the standard normal distribution function, Φ^{-1}. The limit state function can be expressed in terms of the ultimate resistance, R_u, determined through spatial stochastic FEA that includes the effect of self-weight, and the corresponding model error statistics, ME, as well as the out-of-plane wind loading, W_p.

$$G(X) = ME \times R_u - W_p \quad (5)$$

3.2. Calculation of Structural Reliability

The AS 3700 vertical bending moment capacity for simply supported walls with low axial load is:

$$M_{cv} = \phi f_{mt}^{'} Z_d + f_d Z_d \tag{6}$$

where Z_d is the section modulus per metre wall length, f_d is the design compressive stress, and $f_{mt}^{'}$ is the design flexural tensile bond strength.

The design flexural tensile bond strength is based on two values defined in AS 3700: (i) a characteristic flexural tensile bond strength not greater than 0.2 MPa and (ii) a 5th percentile (characteristic) strength value calculated from bond strength measurements. For example, for Cases 1, 3 and 4 this equates to $f_{mt}^{'}$ = 0.14 MPa (see Table 1). Both values have been considered in this analysis to account for the most critical design case, whereby the characteristic flexural tensile bond strength is overestimated in the absence of test data by considering the limiting value of 0.2 MPa.

The nominal resistance is calculated for a simply supported wall in one-way bending is:

$$R_n = \frac{M_{cv} 8}{H^2} = \frac{\left(\phi f_{mt}^{'} Z_d + f_d Z_d\right) 8}{H^2} \tag{7}$$

where the overall wall height is H = 2408 mm, and the minimum design compressive stress on the bed joint at the location of flexural cracking is calculated as the effect of the self-weight at mid-height of the wall is:

$$f_d = 0.5 \gamma H \tag{8}$$

where the mean bulk density (γ) is 19 kN/m^3 (AS 3700 2018) and the COV is 0.02 following a normal distribution (Lawrence and Stewart 2009).

The nominal resistances when ϕ = 1.0 are 0.45 kPa and 0.62 kPa when $f_{mt}^{'}$ = 0.14 MPa and $f_{mt}^{'}$ = 0.2 MPa, respectively. The mean values from the SFEAs (see Table 3) are about 1.2 kPa – i.e., mean(R_u/R_n) = 1.94 – this suggests, as expected, that there is significant reserve capacity in the walls.

The mean-to-nominal statistics for peak annual wind loading for non-cyclonic and cyclonic conditions are based on recommendations from the Australian Building Codes ABCB (2019), see Table 4. The superseded wind load statistics proposed by Pham (1985) are significantly lower than the ABCB wind loading statistics (Stewart 2018). The wind load statistics are related to nominal resistance as:

$$W_p = R_n \frac{W}{W_n} \tag{9}$$

The probability of failure is thus:

$$\begin{aligned} p_f &= Pr\left[ME \times R_u - R_n \times \frac{W_{mean}}{W_n} \leq 0\right] \\ &= Pr\left[ME \times R_u - \frac{\left(\phi f_{mt}^{'} Z_d + 0.5 \gamma H Z_d\right) 8}{H^2} \times \frac{W}{W_n} \leq 0\right] \end{aligned} \tag{10}$$

where ME, R_u, γ, and W/W_n are modelled as random variables (see Tables 3 and 4), and all other parameters are deterministic.

3.3. Target Reliability

The Australian Standard 'General principles on reliability for structures' AS 5104 (2017), (adopted from ISO 2394 (2015)), provides a basis for determining the target annual reliability (β_T) which can be used to assess the capacity reduction factor. The target reliability is selected by considering several factors including the nature of failure, the expected costs associated with failure, and the cost associated with reducing the probability of failure. The nature of failure is critical in the determination of target reliability. Structural elements that exhibit brittle or sudden failure should be assessed in a higher consequence class than those for which collapse is more gradual. The ability to mitigate the effects of failure reduces the necessary consequence class. Unreinforced masonry walls subjected to one-way vertical bending exhibit brittle failure without pre-warning.

Table 4. Statistical parameters W/W_n for peak annual wind loading ABCB (2019).

Conditions	Mean	COV	Distribution
Non-cyclonic	0.33	0.49	Lognormal
Cyclonic	0.16	0.71	Lognormal

Table 5. Annual target reliabilities (β_T) for economic optimisation (adapted from JCSS 2021, AS 5104 2017).

	Consequence of Failure		
Relative Costs of Safety Measures	Class 2 (Minor)	Class 3 (Moderate)	Class 4 (Large)
Large	3.1	3.3	3.7
Medium	3.7	4.2	4.4
Small	4.2	4.4	4.7

The present design situation is a single skin infill masonry panel subject to a lateral (wind) load – i.e., there is no vertical pre-compression other than panel self-weight. In this case, the consequence class is initially classified as Class 2 (expected number of fatalities fewer than 5, smaller buildings and industrial facilities); however, as the failure mode is non-ductile without pre-warning the consequence class is increased to Class 3 (moderate consequences of failure – material losses and functionality losses of societal significance, expected number of fatalities fewer than 50, most residential buildings) in Table 5. The Joint Committee on Structural Safety Probabilistic Model Code (JCSS 2021) recommends that the relative cost of safety is medium for '*the most common design situation*'. Moreover, JCSS (2021) states that *'a large uncertainty in either loading or resistance (coefficients of variation larger than 40%) . . . a lower reliability class should be used. The point is that for these large uncertainties the additional costs to achieve a high reliability are prohibitive.*' As noted in Table 4, the COV of peak annual wind load reaches 0.49. Hence, for a minor consequence Class 2 and medium relative cost of safety measures the annual target reliability index is $\beta_T = 3.7$ ($p_f = 1.1 \times 10^{-4}$). A moderate consequence (Class 3) would increase the target reliability index to $\beta_T = 4.2$ ($p_f = 1.3 \times 10^{-5}$).

A Class 4 consequence would be a disastrous event causing disruptions and delays at a national scale over periods in the order of months, with the expected number of fatalities being fewer than 500. If such a large consequence is considered, then the target reliability index increases to $\beta_T = 4.4$ ($p_f = 5.4 \times 10^{-6}$). Given the additional limitations imposed on the use of unreinforced masonry in AS 3700 (2018) this level of consequence is not deemed relevant.

3.4. Discretisation of Thickness

It is recognised that bricks are manufactured in discrete sizes and so designers will normally adjust support conditions, span lengths and structural systems to optimise unit thickness selection. However, it is most likely that the unit thickness will still need to be 'rounded-up' (i.e., discrete size greater than the design thickness). This 'rounding-up' may be incorporated into a reliability analysis by increasing the wall thickness, and the increase in structural reliability is significant (Stewart and Lawrence 2002). This phenomenon occurs also for reinforced concrete and structural steel sections where the mean over-sizing is estimated to be approximately 5% (e.g., Melchers and Beck 2018). However, reliability-based code–calibration studies usually ignore this influence and so it is also not considered in the present study. It should be noted, however, that ignoring this influence is conservative, and this effect is potentially higher for masonry than for other materials.

3.5. Results for Cases 1-4

A structural reliability analysis was initially completed for an URM wall 2.408 m high and 2.4 m in length in one-way vertical bending for the benchmark Case 1. Considering the capacity reduction factor specified in AS 3700 (2018) ($\phi = 0.6$), for Case 1 when the calculated characteristic strength (0.14 MPa) was used to design the URM wall, the annual reliability index was found to be 5.04 for non-cyclonic and cyclonic conditions. When the AS 3700 (2018) characteristic strength value (0.20 MPa) is used to calculate the design strength, the annual reliability index values decreases to 4.47 and 4.61 for non-cyclonic and cyclonic

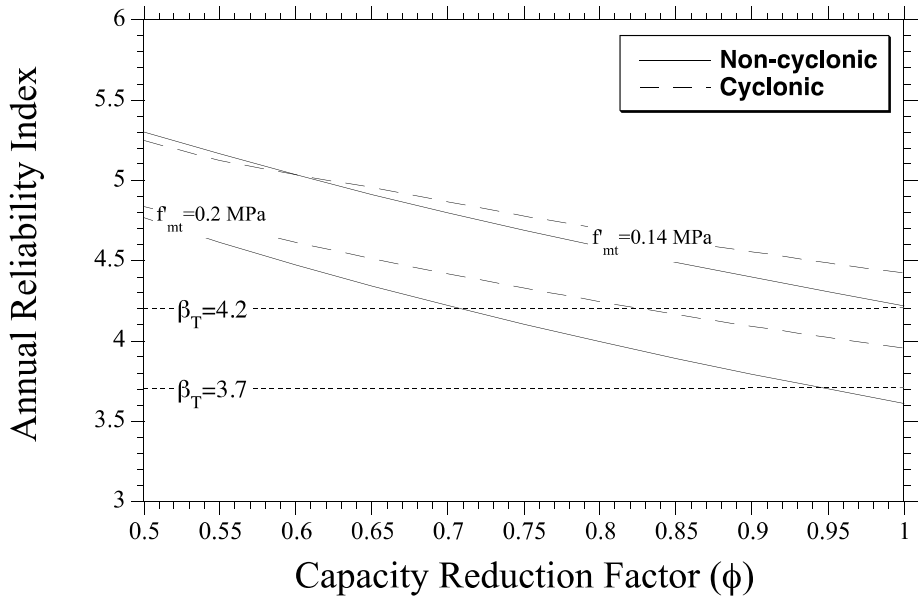

Figure 8. Effect of capacity reduction factor on reliability index for Case 1.

conditions, respectively. The relationship between the capacity reduction factor and the reliability index for non-cyclonic and cyclonic conditions is shown in Figure 8. A wall designed to the AS 3700 (2018) recommended characteristic flexural tensile bond strength of f'_{mt}= 0.2 MPa results in a lower design thickness compared to the one designed to the 5th percentile of the bond strength distribution (f'_{mt}= 0.14 MPa) for the same design load. Hence, it is evident from Figure 8 that designing to f'_{mt} = 0.2 MPa leads to a lower reliability and is thus the governing case.

In Figure 8 it is also shown than an URM wall designed for one-way bending exceeds the target reliabilities for all values of ϕ if designed to f'_{mt} = 0.14 MPa. On the other hand, the capacity reduction factor (ϕ) needed to meet the target reliabilities for f'_{mt} = 0.2 MPa are 0.95 and 0.70 for β_T = 3.7 and β_T = 4.2, respectively, for non-cyclonic regions. If a higher target reliability of β_T = 4.4 is selected, then ϕ = 0.63 for non-cyclonic regions. For the cyclonic regions, the ϕ values are higher for all target reliabilities.

It might appear counter-intuitive that reliabilities are mostly lower for non-cyclonic regions. This is not to mean that non-cyclonic wind speeds are higher, but that the actual mean wind speeds are proportionally higher than the nominal (design) values for non-cyclonic regions mean(W/W_n) = 0.33 than they are for cyclonic regions where mean(W/W_n) = 0.16. This is offset, in part, by the significantly higher variability of cyclonic winds. In other words, nominal design wind speeds for non-cyclonic regions may be slightly less conservative when compared to cyclonic regions.

Since designing to the AS 3700 (2018) recommended characteristic flexural tensile bond strength of f'_{mt} = 0.2 MPa leads to lower reliabilities, the results and discussion to follow will focus on this conservative design criteria.

A reliability-based calibration of AS 3700 (2018) is completed considering target annual reliability index values of 3.7 and 4.2. The capacity reduction factors determined for the non-cyclonic and cyclonic conditions are given in Table 6 for Cases 1 to 4. The effect of determining the bond strength probability distribution based on 0.2 MPa being the 5th percentile (Case 2) increases reliabilities slightly, leading to a slightly higher ϕ value. A shorter wall length (Case 3) results in a reliability index only 0.01 lower than the benchmark Case 1. A longer wall has more opportunity for load redistribution, leading to higher mean resistance and lower variability (e.g., Isfeld, Stewart, and Masia 2021), leading to a higher reliability. Considering all cases, the lowest (critical) ϕ value is 0.70 (Non-cyclonic, Case 3).

To be conservative, it may be recommended that the capacity reduction factor be increased from the current AS3700 value of ϕ = 0.6 to ϕ = 0.65. In this case, the minimum annual reliability index is 4.32 (Non-cyclonic, Case 3) which easily exceeds the strictest target reliability of β_T = 4.2.

3.6. Sensitivity Analyses

The sensitivity of the reliability analysis to critical factors is tested by adjusting those factors and comparing the results to benchmark Case 1 with a design bond strength of 0.2 MPa and for ϕ = 0.6. Factors of interest include variability of self-weight, variability of model error, change in unit thickness, and probabilistic distributions for model error, bond strength, and ultimate resistance.

Table 7 shows the reliability indices when (i) self-weight is treated as deterministic, (ii) unit thickness is rounded up by 5%, (iii) model error is treated as deterministic equal to 1.0, and (iv) model error has a mean of 1.0 and COV of 0.05, (v) flexural bond strength is lognormal or Weibull as suggested by some other researchers (Lawrence 1983, 1985), (v) ultimate resistance distribution is evaluated with the distribution found to have the second best fit (Weibull), and (vii) flexural bond strength statistics based on a 5th percentile of 0.2 MPa and a COV = 0.5 (mean = 0.746 MPa, COV = 0.5).

As expected, a deterministic self-weight has a negligible effect on the calculated reliability. This is

Table 6. Capacity reduction factor (ϕ) for target annual reliability index of 3.7 and 4.2, for Cases 1–4 and f'_{mt} = 0.2 MPa.

		Capacity Reduction Factor (ϕ) to meet Target Reliability	
	Reliability Index when ϕ = 0.6	β_T = 3.7	β_T = 4.2
Non-cyclonic:			
Case 1	4.47	0.95	0.70
Case 2	4.51	0.96	0.72
Case 3	4.46	0.94	0.70
Case 4	4.57	0.99	0.75
Cyclonic:			
Case 1	4.61	>1	0.83
Case 2	4.63	>1	0.84
Case 3	4.60	>1	0.82
Case 4	4.68	>1	0.87

Table 7. Sensitivity Analysis of Reliability Indices for benchmark Case 1 and f'_{mt} = 0.2 MPa.

	ϕ = 0.6		ϕ = 0.65	
	Non-Cyclonic	Cyclonic	Non-Cyclonic	Cyclonic
Benchmark Case 1	4.47	4.61	4.34	4.51
Self-weight deterministic	4.48	4.61	4.35	4.51
Unit thickness is rounded up by 5%	4.68	4.76	4.54	4.67
Model error mean(ME) =1.0, COV(ME) =0.0	4.85	4.84	4.71	4.74
Model error mean(ME) =1.0, COV(ME) =0.05	4.82	4.82	4.68	4.72
Flexural bond strength is Weibull distribution: mean(R_u) =1.16 kPa, COV(R_u) =0.11	4.40	4.55	4.26	4.45
Flexural bond strength is lognormal distribution: mean(R_u) =1.25 kPa, COV(R_u) =0.08	4.61	4.70	4.48	4.60
Flexural bond strength: mean = 0.746 MPa, COV =0.5: mean(R_u) =1.51 kPa, COV(R_u) =0.12	4.87	4.93	4.74	4.83
Ultimate resistance is Weibull distribution	4.41	4.58	4.28	4.48

consistent with the results of Lawrence and Stewart (2011). Considering a deterministic model error of 1.0 or a mean model error of 1.0 and COV of 0.05 had a similar effect for all cases. When the COV of the model error is reduced, the reliability index increased consistently despite the small reduction in the mean model error used in these cases. For Case 1 changing the resistance distribution from normal to Weibull led to a reduction in the reliability index as the Weibull distribution overestimated the probability of low peak pressure values. Changing the flexural bond strength from normal to lognormal increases reliabilities, whereas selecting a Weibull distribution results in a small decrease in the reliability index.

Table 7 also shows the effect of discretisation of unit thickness. For example, if the unit thickness is rounded up by only 5%, then the reliability index increases from 4.47 to 4.68. This shows the important effect that discretising of unit thickness can have on structural reliability. However, as discussed in Section 3.4, reliability-based code–calibration studies usually ignore this influence and so it is not considered in the present study when proposing capacity reduction factors.

In summary, Table 7 shows that the annual reliability indices all exceed the strictest target reliability of β_T = 4.2.

A lower wall height will have less opportunity for low bond strengths as high stresses will occur over fewer courses. For example, for a wall of 1.2 m height, the flexural stresses three courses above mid-height are 85% of the peak (mid-height) stress including self-weight, whereas for a 2.4 m high wall this proportion increases to 96%. This should lead to higher mean-to-nominal capacity (R_u/R_n) and lower COV of peak wall strength for walls lower than 2.4 m in height. URM walls are rarely higher than a single storey of 2.4 m but may reach 3.0 m in some cases. In this case, a slightly lower mean-to-nominal capacity and higher COV of peak wall strength are expected, with a small reduction in reliability.

4. Conclusions and recommendations

A spatial stochastic FEA model was developed to estimate the resistance of full scale URM walls in one-way vertical bending. This model accounts for the unit-to-unit spatial variability of material properties, considering bond strengths observed in typical Australian construction. The walls are subject to a wind load and self-weight with no vertical pre-compression. An established method of structural reliability analysis was applied using the spatial stochastic FEA as a resistance model, considering the random variability of model error, flexural bond strength, and wind load.

The reliability analysis includes a number of assumptions that lead to conservative (lower) reliability indices, namely:

(1) discretisation of unit thickness is not considered – yet its effect would be higher for masonry than other materials.
(2) variability of flexural tensile strength was not reduced to account for variability in bond wrench test procedures.
(3) a design bond strength of 0.2 MPa is used, rather than the calculated 5th percentile obtained from the probability distribution of flexural bond strength.
(4) walls are assumed to be simply supported, whereas in many practical cases there may be partial rotational restraint at the top or bottom of a vertically spanning wall panel.

The reliability indices will be higher if even one of these conservative assumptions were not included in the analysis or were modelled more accurately. Comparison of the annual reliability index to target reliabilities recommended by Australian and

international standards found that the capacity reduction factor for the Australian Standard for Masonry Structures AS 3700 may be increased from $\phi = 0.6$ to $\phi = 0.65$ as the lowest (critical) ϕ value is 0.70. It is therefore reasonable, and still conservative, to round down this value to $\phi = 0.65$ for URM in one-way vertical bending. The robustness of this recommendation is shown through sensitivity analyses. If such a recommendation is implemented in AS 3700, then this will result in an 8.3% increase in the flexural design capacity in the design of new structural masonry in Australia.

Coupling the results of physical wall testing with that of spatial stochastic FEA models has been shown to produce a reliable prediction of the strength distribution of masonry walls. The use of such models in reliability analysis has provided an economical means of evaluating design standards. This approach could be applied to consider the effect of vertical pre-compression on such walls, as well as the effects of two-way bending.

Acknowledgments

The support of the Australian Research Council grant DP180102334 is gratefully acknowledged.

Disclosure statement

No potential conflict of interest was reported by the author(s).

Funding

This work was supported by the Australian Research Council [DP180102334].

References

ABCB. 2019. *Handbook: Structural Reliability Verification Method*. Australian Building Codes Board: Canberra. ACT

Aggregui-Mena, J.D., L. Margetts, and P.M. Mummery. 2016. "Practical Applications of the Stochastic Finite Element Method." *Archives of Computational Methods in Engineering* 23 (1): 171–190.

Argarwal, A., S Foster, and M.G. Stewart. 2021. "Model Error and Reliability of RC Beams in Shear Designed according to the Modified Compression Field Theory." *Structural Concrete* 22 (6): 3711–3726.

AS 3600. 2018. *Concrete Structures*. Sydney Australia: Standards Australia.

AS 3700. 2018. *Masonry Structures*. Sydney, Australia: Standards Australia.

AS 5104. 2017. *General Principles on Reliability for Structures*. Sydney, Australia: Standards Australia.

Baker, L.R. 1981. "The Flexural Action of Masonry Structures under Lateral Load." In *PhD Thesis School of Engineering and Architecture*, 247. Melbourne, Australia: Deakin University.

DIANA FEA BV. 2017. *DIANA 10.2 Finite Element Analysis User's Manual*, edited by Jonna Manie and Gerd-Jan Schreppers, The Netherlands: Delft.

Heffler, L. 2009. "Variability of Unit Flexural Bond Strength and Its Effect on Strength in Clay Brick Unreinforced Masonry Walls Subjected to Vertical Bending." In *MSc Thesis Faculty of Engineering and Built Environment*, 168. Newcastle, Australia: University of Newcastle.

Heffler, L.M., M.G. Stewart, M.J. Masia, and M.R.S. Correa. 2008. "Statistical Analysis and Spatial Correlation of Flexural Bond Strength for Masonry Walls." *Masonry International* 21 (2): 59–70.

Isfeld, A.C., E. Moradabadi, D.F. Laefer, and N.G. Shrive. 2016. "Uncertainty Analysis of the Effect of Grout Injection on the Deformation of multi-wythe Stone Masonry Walls." *Construction and Building Materials* 126: 661–672. doi:10.1016/j.conbuildmat.2016.09.058.

Isfeld, A.C., M.G. Stewart, and M.J. Masia. 2021. "Stochastic Finite Element Model Assessing Length Effect for Unreinforced Masonry Walls Subjected to One-Way Vertical Bending under Out-of-Plane Loading." *Engineering Structures* 236: 112115. doi:10.1016/j.engstruct.2021.112115.

ISO 2394. 2015. *General Principles on Reliability for Structures*. Geneva: International Organization for Standardization.

JCSS (2021). "*Probabilistic Model Code: Part I –Basis Of Design*." Joint Committee On Structural Safety: https://www.jcss-lc.org/publications/jcsspmc/part_i.pdf Accessed 1 February 2021

Lawrence, S.J. 1983. "Behaviour of Brick Masonry Walls under Lateral Loading." In *PhD Thesis School of Civil Engineering*, 424. Sydney, Australia: University of New South Wales.

Lawrence, S.J. 1985. Random Variations in Brickwork Properties. In 7th IBMaC, Melbourne, Australia, 537–548.

Lawrence, S.J., and M.G. Stewart. 2009. "Reliability-based Calibration of the Capacity Reduction Factor for Design of Masonry in Compression to AS3700." *Australian Journal of Structural Engineering* 9 (2): 97–110. doi:10.1080/13287982.2009.11465013.

Lawrence, S.J., and M.G. Stewart. 2011. "Model Error and Structural Reliability for Unreinforced Masonry Walls in Vertical Bending." *Masonry International* 24 (1): 23–30.

Li, J., M.J. Masia, and M.G. Stewart. 2017. "Stochastic Spatial Modelling of Material Properties and Structural Strength of Unreinforced Masonry in Two-Way Bending." *Structure and Infrastructure Engineering* 13 (6): 683–695. doi:10.1080/15732479.2016.1188125.

Li, J., M.J. Masia, M.G. Stewart, and S.J. Lawrence. 2014. "Spatial Variability and Stochastic Strength Prediction of Unreinforced Masonry Walls in Vertical Bending." *Engineering Structures* 59 (1): 787–797. doi:10.1016/j.engstruct.2013.11.031.

Li, J., M.J. Masia, M.G. Stewart, and S.J. Lawrence. 2016. "Spatial Correlation of Material Properties and Structural Strength of Masonry in Horizontal Bending." *ASCE Journal of Structural Engineering* 142 (11): 04016112. doi:10.1061/(ASCE)ST.1943-541X.0001488.

Liu, W.K., T. Belytschko, and A. Mani. 1986. "Random Field Finite Elements." *International Journal for Numerical*

Methods in Engineering 23 (10): 1831–1845. doi:10.1002/nme.1620231004.

Lourenço, P.B. 1996. Computational Strategies for Masonry Structures. *PhD Thesis Civil Engineering and Geosciences*, 210. Delft, The Netherlands: Delft Technical University.

Lourenço, P.B., and J.G. Rots. 1997. "Multisurface Interface Model for Analysis of Masonry Structures." *Journal of Engineering Mechanics-ASCE* 123 (7): 660–668. doi:10.1061/(ASCE)0733-9399(1997)123:7(660).

Lourenço, P.B., J.G. Rots, and J. Blaauwendraad. 1995. "Two Approaches for the Analysis of Masonry Structures: Micro and macro-modelling." *HERON* 40 (4): 313–340.

McNeilly, T., J. Scrivener, S.J. Lawrence, and S. Zsembery. 1996. "A Site Survey of Masonry Bond Strength." *Australian Civil/Structural Engineering Transactions* 38 (2/3/4): 103–109.

McNeilly, T., J. Scrivener, S. Zsembery, and S.J. Lawrence. 1991. "Bond Strength and the Australian Masonry Code." in *9th International Brick and Block Masonry Conference*, Berlin, Germany, 301–307.

Melchers, R.E., and A.T. Beck. 2018. *Structural Reliability Analysis and Prediction*. Chichester, U.K: Wiley.

Milani, G., and P. B. Lourenço. 2013. "Simple Homogenized Model for the Nonlinear Analysis of FRP-Strengthened Masonry Structures. II." *Structural Applications, Journal of Engineering Mechanics-Asce* 139 (1): 77–93. doi:10.1061/(ASCE)EM.1943-7889.0000479.

Moradabadi, E., D. F. Laefer, J. A. Clarke, and P. B. Lourenco. 2015. "A Semi-Random Field Finite Element Method to Predict the Maximum Eccentric Compressive Load for Masonry Prisms." *Construction and Building Materials* 77: 489–500. doi:10.1016/j.conbuildmat.2014.12.027.

Petersen, R.B., N. Ismail, M.J. Masia, and J.M. Ingham. 2012. "Finite Element Modelling of Unreinforced Masonry Shear Wallettes Strengthened Using Twisted Steel Bars." *Construction and Building Materials* 33: 14–24. doi:10.1016/j.conbuildmat.2012.01.016.

Pham, L. 1985. "Load Combinations and Probabilistic Load Models for Limit States Codes." *Civil Engineering Transactions, IEAust* CE27 (1): 62–67.

Raphael, J.M. 1984. "Tensile Strength of Concrete." *ACI Journal* 81 (2): 158–165.

Stewart, M.G. 2018. "Stochastic Wind Field Models and Their Effect on the Structural Reliability of Masonry Walls." *25th Australasian Conference on Mechanics of Structures and Materials (ACMSM25)*, C.M. Wang, J. C.M. Ho, and S. Kitipornchai (Eds.), Brisbane, Springer.

Stewart, M.G., S. Foster, S. Ahammed, and V. Sirivivatnanon. 2016. "Calibration of Australian Standard AS3600 Concrete Structures, Part II: Reliability Indices and Changes to Capacity Reduction Factors." *Australian Journal of Structural Engineering* 17 (4): 254–266. doi:10.1080/13287982.2016.1246215.

Stewart, M.G., and S.J. Lawrence. 2002. "Structural Reliability of Masonry Walls in Flexure." *Masonry International* 15 (2): 48–52.

Stewart, M.G., and M.J. Masia. 2019. "Reliability-based Assessment of Safety Factors for Masonry Walls in Vertical Bending." In *13th North American Masonry Conference*, Salt Lake City, Utah. p. 12.

Van Der Pluijm, R. 1997. "Non-linear Behaviour of Masonry under Tension." *HERON* 42: 25–54.